AIAA SciTech Forum
7-11 January 2019, San Diego, California
AIAA Scitech 2019 Forum

10.2514/6.2019-1291

Control Design for an Aerial Manipulator for Pick-and-Place Tasks

Donglei Sun* Neng Wan† and Naira Hovakimyan‡
University of Illinois at Urbana-Champaign, Urbana, IL 61801, USA

Weichen Dai§ and Yu Zhang¶
Zhejiang University, Hangzhou, Zhejiang 310027, China

This paper presents a control architecture for an aerial manipulator operating in indoor environments. The objective is to provide a viable solution to the growing need for indoor assistive technology. The study tries to address the problem of payload pick-and-place with unknown mass. The control structure consists of *i*) a baseline pitch angle tracking controller that provides satisfactory performance for the quadrotor without a payload; *ii*) an adaptive augmentation that compensates for the disturbance in the rotational dynamics due to the unknown payload; *iii*) a horizontal position tracking controller that generates the pitch angle command; *iv*) a baseline vertical position tracking controller; and *v*) another adaptive augmentation controller that compensates for the disturbance in the vertical motion from the pick-and-place of the unknown payload. Since the robotic manipulator operates in the vertical plane of symmetry of the quadrotor, the control design is considered for the motion only in this plane. The controller is verified in a simulation environment.

I. Introduction

Aerial robots hold a great promise to help older population in their daily activities and facilitate the "aging in place" [1–3]. Among several types of daily activities, study shows that fetching objects from the floor or another room is one of those that are preferred to be completed by robots [4]. In [5] an aerial vehicle appropriate for indoor use was designed and augmented with a manipulator so that it can pick up common household items such as medicine bottles, reading glasses, and cell phones, for people with reduced mobility. The vehicle is shown in Fig. 1. This type of small aerial vehicles are agile and have the advantage in completing this sort of task over ground vehicles, which are not capable of climbing stairs or reaching for items at high altitudes. However, the control design poses a great challenge due to uncertainties, such as the objects that it picks up, and the coupling between the manipulator and the quadrotor. In [5], an adaptive control structure was designed to compensate for the torque due to an unknown payload, where only the rotational motion was considered, while the influence of the unknown payload on the translational motion of the vehicle during the pick-and-place mission was not addressed. In this study, control laws are designed to achieve stable pick-and-place missions.

During the past decade, aerial manipulators have attracted wide attention of researchers. The study in [6] presents design of several light-weight, low-complexity grippers that allow UAVs to pick up and transport a wide range of payloads; however, the vehicle is required to fly directly over the top of the payload. An algorithm for aerial grasping of moving targets is presented in [7], where two classes of grasping maneuvers are discussed, and a planning strategy based on differential flatness is proposed. However, the single link design of this aerial manipulator imposes restrictions on the work space, and the payload cannot be moved close to the center of mass of the vehicle, creating challenges for navigation through narrow passages. In [8], a quadrotor with a 2-link manipulator is introduced, enabling the end-effector to achieve arbitrary orientation and overcome the drawbacks with grippers fixed to a quadrotor. A controller based on feedback linearization is designed for trajectory tracking. References [9] and [10] present a design, where a quadrotor MAV is equipped with an actuated appendage to enable grasping and retrieval of objects at high speeds, and differential flatness property is used in dynamic trajectory planning. A Lyapunov-based model reference adaptive

*Doctoral Student, Dept. of Aerospace Engineering, Student Member AIAA; dsun13@illinois.edu.
†Doctoral Student, Dept. of Mechanical Science and Engineering; nengwan2@illinois.edu.
‡Professor, Dept. of Mechanical Science and Engineering, Fellow AIAA; nhovakim@illinois.edu.
§Doctoral Student, College of Control Science and Engineering; weichendai@zju.edu.cn
¶Associate Professor, College of Control Science and Engineering; zhangyu80@zju.edu.cn

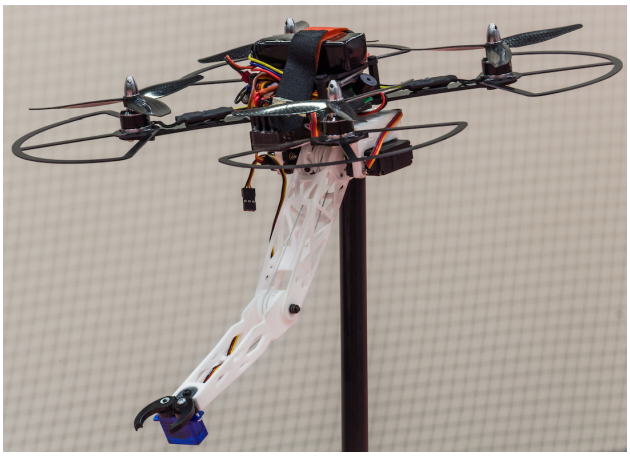

Fig. 1 An aerial manipulator designed as an indoor assisting system

control design for aerial manipulation is presented in [11] for an aerial vehicle with dual manipulators. A control system based on feedback linearization and PD control for an aerial manipulator is proposed in [12], taking into account the mutual reactive influence between the robotic manipulator and the UAV. In [13], a six degree of freedom parallel manipulator that can robustly maintain precise end-effector positioning in the presence of perturbations is designed. For unknown payload, [14] presents an on-line estimator to evaluate the unknown payload, and a passivity-based control algorithm is designed for the system. The study in [15] introduces a nonlinear model predictive control methodology to achieve optimized performance in pick-and-place tasks of aerial manipulators, by employing a sequential Newton method for unconstrained optimal control and a high-frequency low-level controller for optimal trajectory tracking. On-board vision system is used for object finding. In [16], a quadcopter equipped with a Delta-type parallel manipulator was studied, and an $\mathcal{L}_1$ adaptive controller was designed to augment the baseline control law for rotational motion.

In this paper, we will discuss the control design for vehicle stabilization during object manipulations. Due to the coupling between the robotic manipulator and the quadrotor, operations of the manipulator will influence the system dynamic properties remarkably, such as the center of mass and moment of inertia, among others. To reduce its effect, in this study it is assumed that the robot arm keeps its configuration during the pick-and-place mission. In addition to the robot arm, the uncertainty caused by various objects to be picked up is also considered in the system dynamics. To stabilize the whole system and guarantee satisfactory manipulation performance, a pitch angle controller will be designed as the inner-loop of the horizontal position controller. A vertical position controller will also be designed to follow the vertical position command. To compensate for the disturbance induced by the robotic arm and the unknown payload, two $\mathcal{L}_1$ adaptive controllers are proposed as augmentation to the baseline controllers, one for the rotational motion and the other for the vertical translational motion. $\mathcal{L}_1$ adaptive controllers have been implemented in a large number of flight tests, involving various uncertainties, including mass change, component failures, and disturbances [17–21]. Since during the process of pick-and-place, the vehicle's motion is mainly in the vertical plane of symmetry, the modeling work and control design presented here will be carried out only considering generalized coordinates associated with this plane. Control design will be developed and tested in a simulation environment.

This paper is organized as follows. Section II presents the mathematical model of the aerial manipulator in the vertical plane of symmetry. In Section III the control design of the system is discussed. Simulation results are presented in Section IV. Finally Section V concludes the paper.

II. Mathematical Model of the Aerial Manipulator

In this section, the mathematical model of the aerial manipulator will be derived for control design purposes. During the process of object pick-and-place, the motion takes place in the vertical plane of symmetry of the vehicle. Hence the equations of motion of the system in this plane will be explored using Lagrangian dynamics. Several coordinate systems are defined to facilitate the modeling process of the system, and they are shown in Fig. 2a. The world frame $\{o_e\}$ is an inertial frame, and the body frame $\{o_1\}$ is fixed at the center of mass of the quadrotor. Assume that the joint (joint 1) between the quadrotor and link 1 of the manipulator is located at the center of mass of the quadrotor, and the joint

rotates about y_1-axis. The frame $\{o_2\}$ is fixed at the end of link 1 with z_2-axis aligned with link 1, and joint 2 rotates about y_2-axis. The frame $\{o_3\}$ is fixed at the end of link 2 with z_3-axis along link 2. A diagram of the system with coordinate frames in the plane of symmetry is shown in Fig. 2b. Note that the center of mass of the payload coincides with the origin of $\{o_3\}$.

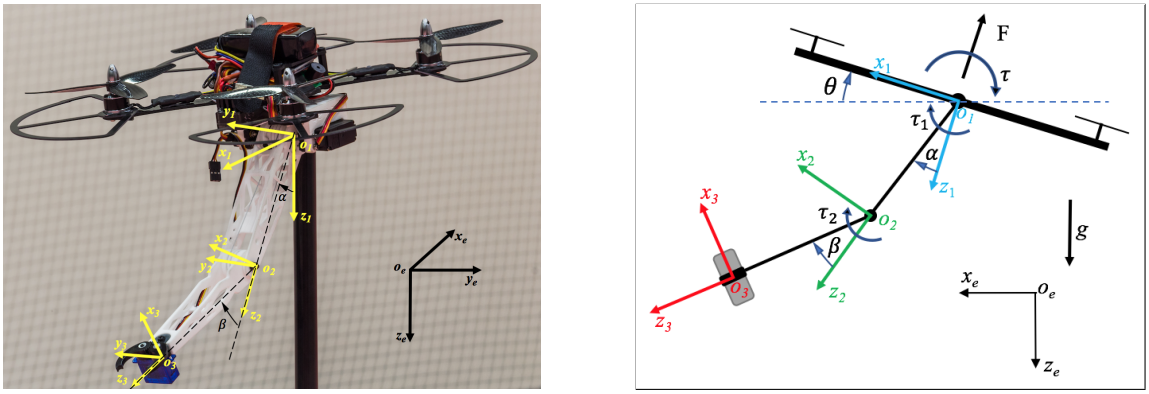

(a) Coordinate systems **(b) Diagram of the system in the plane of symmetry**

Fig. 2 The aerial manipulator and coordinate systems used in modeling

Choose the following generalized coordinates $\bar{q} = \left[x_q, z_q, \theta, \alpha, \beta\right]^\top$, where x_q and z_q are the coordinates of the center of mass of the quadrotor in the inertial frame $\{o_e\}$, θ is the pitch angle of the quadrotor, and α and β are the two joint angles as shown in Fig. 2b. With this set of generalized coordinates, the generalized force will be

$$Q(\bar{q}) = \begin{bmatrix} -F\sin\theta \\ -F\cos\theta \\ \tau \\ \tau_1 \\ \tau_2 \end{bmatrix},$$

where F and τ are the total force and torque generated by the propellers of the quadrotor, and τ_1 and τ_2 are the joint torques. The kinetic energy of the system, carrying a payload of mass m_p and having moment of inertia I_{yyp} about y_3-axis, can be written as

$$\begin{aligned} T = &\frac{1}{2}m_1(\dot{x}_q^2 + \dot{z}_q^2) + \frac{1}{2}m_2\left\{\dot{x}_q^2 + \dot{z}_q^2 + l_{c1}^2(\dot{\theta}+\dot{\alpha})^2 + 2l_{c1}\left[\cos(\theta+\alpha)\dot{x}_q - \sin(\theta+\alpha)\dot{z}_q\right](\dot{\theta}+\dot{\alpha})\right\} \\ &+ \frac{1}{2}m_3\left\{\dot{x}_q^2 + \dot{z}_q^2 + l_1^2(\dot{\theta}+\dot{\alpha})^2 + l_{c2}^2(\dot{\theta}+\dot{\alpha}+\dot{\beta})^2 + 2l_1\left[\cos(\theta+\alpha)\dot{x}_q - \sin(\theta+\alpha)\dot{z}_q\right](\dot{\theta}+\dot{\alpha})\right. \\ &\left.+2l_{c2}\left[\cos(\theta+\alpha+\beta)\dot{x}_q - \sin(\theta+\alpha+\beta)\dot{z}_q + l_1\cos(\beta)(\dot{\theta}+\dot{\alpha})\right](\dot{\theta}+\dot{\alpha}+\dot{\beta})\right\} \\ &+ \frac{1}{2}m_p\left\{\dot{x}_q^2 + \dot{z}_q^2 + l_1^2(\dot{\theta}+\dot{\alpha})^2 + l_2^2(\dot{\theta}+\dot{\alpha}+\dot{\beta})^2 + 2l_1\left[\cos(\theta+\alpha)\dot{x}_q - \sin(\theta+\alpha)\dot{z}_q\right](\dot{\theta}+\dot{\alpha})\right. \\ &\left.+2l_2\left[\cos(\theta+\alpha+\beta)\dot{x}_q - \sin(\theta+\alpha+\beta)\dot{z}_q + l_1\cos(\beta)(\dot{\theta}+\dot{\alpha})\right](\dot{\theta}+\dot{\alpha}+\dot{\beta})\right\} \\ &+ \frac{1}{2}I_{yy1}\dot{\theta}^2 + \frac{1}{2}I_{yy2}(\dot{\theta}+\dot{\alpha})^2 + \frac{1}{2}I_{yy3}(\dot{\theta}+\dot{\alpha}+\dot{\beta})^2 + \frac{1}{2}I_{yyp}(\dot{\theta}+\dot{\alpha}+\dot{\beta})^2, \end{aligned}$$

where m_1, m_2, and m_3 denote the mass of the quadrotor (including servomotors and batteries), link 1, and link 2 of the manipulator respectively; l_1 and l_2 represent the lengths of link 1 and 2 of the manipulator; l_{ci} is the distance from the center of mass of the link i to the joint i of the manipulator for $i = 1, 2$; I_{yy1}, I_{yy2}, and I_{yy3} are the moments of inertia about the center of mass of the quadrotor, link 1, and link 2 respectively.

The potential energy of the system can be written as

$$\begin{aligned} V = &- m_1 g z_q - m_2 g\left[z_q + l_{c1}\cos(\theta+\alpha)\right] - m_3 g\left[z_q + l_1\cos(\theta+\alpha) + l_{c2}\cos(\theta+\alpha+\beta)\right] \\ &- m_p g\left[z_q + l_1\cos(\theta+\alpha) + l_2\cos(\theta+\alpha+\beta)\right]. \end{aligned}$$

Then the Lagrangian is $L = T - V$. Using the Lagrangian dynamic equations

$$\frac{\mathrm{d}}{\mathrm{d}t}\left(\frac{\partial L}{\partial \dot{\bar{q}}_i}\right) - \frac{\partial L}{\partial \bar{q}_i} = Q_i(\bar{q}), \quad i = 1, 2, 3, 4, 5,$$

we obtain the following equations of motion

$$M(\bar{q})\ddot{\bar{q}} + C(\dot{\bar{q}}, \bar{q})\dot{\bar{q}} + G(\bar{q}) = Q(\bar{q}), \tag{1}$$

where the matrices $M(\bar{q})$, $C(\bar{q}, \dot{\bar{q}})$, and $G(\bar{q})$ are defined in Eqs. (32)–(33) in Appendix.

In this paper, it is assumed that the configuration of the robot arm is fixed during the flight and object manipulation, and the actuators controlling the joint angle α and β will keep the joint angles unchanged. Hence, we have

$$\ddot{\alpha} = \dot{\alpha} = 0,$$
$$\ddot{\beta} = \dot{\beta} = 0.$$

With this assumption, the reduced model of the system can be written as

$$M_r(\bar{q})\ddot{\bar{q}} + C_r(\dot{\bar{q}}, \bar{q})\dot{\bar{q}} + G_r(\bar{q}) = Q_r(\bar{q}), \tag{2}$$

where the new coordinates $\bar{q} = \begin{bmatrix} x_q, & z_q, & \theta \end{bmatrix}^\top$, and the matrices $M_r(\bar{q})$, $C_r(\dot{\bar{q}}, \bar{q})$, $G_r(\bar{q})$, and $Q_r(\bar{q})$ are defined in Eqs. (3)–(6). In the following section of control design, this reduced model will be used instead of the model in Eq. (1).

$$M_r(\bar{q}) = \begin{bmatrix} m_1 + m_2 + m_3 + m_p & 0 & \begin{array}{l}(m_2 l_{c1} + m_3 l_1)\cos(\theta+\alpha) \\ + m_3 l_{c2}\cos(\theta+\alpha+\beta) \\ + m_p l_1 \cos(\theta+\alpha) \\ + m_p l_2 \cos(\theta+\alpha+\beta)\end{array} \\ 0 & m_1 + m_2 + m_3 + m_p & \begin{array}{l}-(m_2 l_{c1} + m_3 l_1)\sin(\theta+\alpha) \\ - m_3 l_{c2}\sin(\theta+\alpha+\beta) \\ - m_p l_1 \sin(\theta+\alpha) \\ - m_p l_2 \sin(\theta+\alpha+\beta)\end{array} \\ \begin{array}{l}(m_2 l_{c1} + m_3 l_1)\cos(\theta+\alpha) \\ + m_3 l_{c2}\cos(\theta+\alpha+\beta) \\ + m_p l_1 \cos(\theta+\alpha) \\ + m_p l_2 \cos(\theta+\alpha+\beta)\end{array} & \begin{array}{l}-(m_2 l_{c1} + m_3 l_1)\sin(\theta+\alpha) \\ - m_3 l_{c2}\sin(\theta+\alpha+\beta) \\ - m_p l_1 \sin(\theta+\alpha) \\ - m_p l_2 \sin(\theta+\alpha+\beta)\end{array} & \begin{array}{l}I_{yy1} + I_{yy2} + I_{yy3} + I_{yyp} + m_2 l_{c1}^2 \\ + m_3(l_1^2 + l_{c2}^2 + 2 l_1 l_{c2}\cos(\beta)) \\ + m_p(l_1^2 + l_2^2 + 2 l_1 l_2 \cos(\beta))\end{array} \end{bmatrix}, \tag{3}$$

$$C_r(\dot{\bar{q}}, \bar{q}) = \begin{bmatrix} 0 & 0 & \begin{array}{l}-\dot{\theta}\left[(m_2 l_{c1} + m_3 l_1)\sin(\theta+\alpha) + m_3 l_{c2}\sin(\theta+\alpha+\beta)\right] \\ -\dot{\theta}\left[m_p l_1 \sin(\theta+\alpha) + m_p l_2 \sin(\theta+\alpha+\beta)\right]\end{array} \\ 0 & 0 & \begin{array}{l}-\dot{\theta}\left[(m_2 l_{c1} + m_3 l_1)\cos(\theta+\alpha) + m_3 l_{c2}\cos(\theta+\alpha+\beta)\right] \\ -\dot{\theta}\left[m_p l_1 \cos(\theta+\alpha) + m_p l_2 \cos(\theta+\alpha+\beta)\right]\end{array} \\ 0 & 0 & 0 \end{bmatrix}, \tag{4}$$

$$G_r(\bar{q}) = \begin{bmatrix} 0 \\ -(m_1 + m_2 + m_3 + m_p)g \\ \begin{array}{c}(m_2 l_{c1} + m_3 l_1 + m_p l_1)g\sin(\theta+\alpha) \\ + (m_3 l_{c2} + m_p l_2)g\sin(\theta+\alpha+\beta)\end{array} \end{bmatrix}, \tag{5}$$

$$Q_r(\bar{q}) = \begin{bmatrix} -F\sin\theta \\ -F\cos\theta \\ \tau \end{bmatrix}. \tag{6}$$

III. Control Law Design

In this section, the design of control law is discussed. To facilitate the control law design and testing, a Simulink model is built to model the dynamics of the quadrotor and the manipulator. All control designs are tested in this environment. Before we present the general control structure and details of the control design, the mathematical model in Eq. (2) is processed first, and some simplifying assumptions are introduced.

A. Model Simplification and Analysis

In this part, the model presented in Eq. (2) is simplified based on some practical assumptions to facilitate the control design. Since the mass of the picked-up payload is unknown, all three matrices $M_r(\bar{q})$, $C_r(\dot{\bar{q}}, \bar{q})$, and $G_r(\bar{q})$ can be decomposed into two matrices – one contains all the known variables and the other has unknown m_p. Let the superscript k denote *known*, and superscript u denote *unknown*. We can write

$$\begin{aligned} M_r(\bar{q}) &= M_r^k(\bar{q}) + M_r^u(\bar{q}), \\ C_r(\dot{\bar{q}}, \bar{q}) &= C_r^k(\dot{\bar{q}}, \bar{q}) + C_r^u(\dot{\bar{q}}, \bar{q}), \\ G_r(\bar{q}) &= G_r^k(\bar{q}) + G_r^u(\bar{q}), \end{aligned} \tag{7}$$

where

$$\begin{aligned} M_r^k(\bar{q}) &= M_r(\bar{q})|_{m_p=0}, \\ C_r^k(\dot{\bar{q}}, \bar{q}) &= C_r(\dot{\bar{q}}, \bar{q})\Big|_{m_p=0}, \\ G_r^k(\bar{q}) &= G_r(\bar{q})|_{m_p=0}, \\ M_r^u(\bar{q}) &= M_r(\bar{q}) - M_r^k(\bar{q}), \\ C_r^u(\dot{\bar{q}}, \bar{q}) &= C_r(\dot{\bar{q}}, \bar{q}) - C_r^k(\dot{\bar{q}}, \bar{q}), \\ G_r^u(\bar{q}) &= G_r^u(\bar{q}) - G_r^k(\bar{q}). \end{aligned}$$

The matrices $M_r^u(\bar{q})$, $C_r^u(\dot{\bar{q}}, \bar{q})$, and $G_r^u(\bar{q})$ can be written as

$$M_r^u(\bar{q}) = \left[\begin{array}{c|c|c} m_p & 0 & \begin{array}{l} m_p l_1 \cos(\theta+\alpha) \\ +m_p l_2 \cos(\theta+\alpha+\beta) \end{array} \\ \hline 0 & m_p & \begin{array}{l} -m_p l_1 \sin(\theta+\alpha) \\ -m_p l_2 \sin(\theta+\alpha+\beta) \end{array} \\ \hline \begin{array}{l} m_p l_1 \cos(\theta+\alpha) \\ +m_p l_2 \cos(\theta+\alpha+\beta) \end{array} & \begin{array}{l} -m_p l_1 \sin(\theta+\alpha) \\ -m_p l_2 \sin(\theta+\alpha+\beta) \end{array} & \begin{array}{l} I_{yyp} \\ +m_p(l_1^2 + l_2^2 + 2l_1 l_2 \cos(\beta)) \end{array} \end{array}\right], \tag{8}$$

$$C_r^u(\dot{\bar{q}}, \bar{q}) = \left[\begin{array}{c|c|c} 0 & 0 & -\dot{\theta} m_p \left[l_1 \sin(\theta+\alpha) + l_2 \sin(\theta+\alpha+\beta)\right] \\ \hline 0 & 0 & -\dot{\theta} m_p \left[l_1 \cos(\theta+\alpha) + l_2 \cos(\theta+\alpha+\beta)\right] \\ \hline 0 & 0 & 0 \end{array}\right], \tag{9}$$

$$G_r(\bar{q}) = \left[\begin{array}{c} 0 \\ \hline -m_p g \\ \hline m_p l_1 g \sin(\theta+\alpha) + m_p l_2 g \sin(\theta+\alpha+\beta) \end{array}\right]. \tag{10}$$

Note that when $m_p = 0$, the three matrices become zero. If we assume that the object is a regular cylinder, then I_{yyp} is proportional to m_p, and m_p can be factored out in all above three matrices. With those matrices defined in Eq. (7), the

dynamic equations of the system in Eq. (2) can be written as

$$\left[M_r^k(\bar{q}) + M_r^u(\bar{q})\right]\ddot{\bar{q}} + \left[C_r^k(\dot{\bar{q}},\bar{q}) + C_r^u(\dot{\bar{q}},\bar{q})\right]\dot{\bar{q}} + \left[G_r^k(\bar{q}) + G_r^u(\bar{q})\right] = Q_r(\bar{q}). \tag{11}$$

Since $M_r(\bar{q})$ is always symmetric and invertible, we obtain

$$\ddot{\bar{q}} = \left[M_r^k(\bar{q}) + M_r^u(\bar{q})\right]^{-1}\left(-\left[C_r^k(\dot{\bar{q}},\bar{q}) + C_r^u(\dot{\bar{q}},\bar{q})\right]\dot{\bar{q}} - \left[G_r^k(\bar{q}) + G_r^u(\bar{q})\right] + Q_r(\bar{q})\right). \tag{12}$$

Based on the matrix inversion equality in [22], the inversion of the sum of two matrices can be represented by

$$\left[M_r^k(\bar{q}) + M_r^u(\bar{q})\right]^{-1} = \left[M_r^k(\bar{q})\right]^{-1} - \underbrace{\left[M_r^k(\bar{q})\right]^{-1}\left(\mathbb{I} + M_r^u(\bar{q})\left[M_r^k(\bar{q})\right]^{-1}\right)^{-1} M_r^u(\bar{q})\left[M_r^k(\bar{q})\right]^{-1}}_{=:M_r^{u2}(\bar{q})}.$$

Let the second term in the above equation be denoted by $M_r^{u2}(\bar{q})$, which can be seen as a correction to the inverse of $M_r^k(\bar{q})$ due to $M_r^u(\bar{q})$ induced by the unknown payload m_p. Then we can write

$$\left[M_r^k(\bar{q}) + M_r^u(\bar{q})\right]^{-1} = \left[M_r^k(\bar{q})\right]^{-1} - M_r^{u2}(\bar{q}).$$

Note that if $m_p = 0$, then $M_r^u(q) = \mathbf{0}$, and hence $M_r^{u2}(\bar{q}) = \mathbf{0}$. With this, the equation of motion in Eq. (12) can be written as

$$\begin{aligned}\ddot{\bar{q}} &= \left(\left[M_r^k(\bar{q})\right]^{-1} - M_r^{u2}(\bar{q})\right)\left(-\left[C_r^k(\dot{\bar{q}},\bar{q}) + C_r^u(\dot{\bar{q}},\bar{q})\right]\dot{\bar{q}} - \left[G_r^k(\bar{q}) + G_r^u(\bar{q})\right] + Q_r(\bar{q})\right)\\ &= -\left[M_r^k(\bar{q})\right]^{-1}\left(C_r^k(\dot{\bar{q}},\bar{q})\dot{\bar{q}} + G_r^k(\bar{q}) + Q_r(\bar{q})\right) - W(m_p,\dot{\bar{q}},\bar{q}).\end{aligned} \tag{13}$$

In above equation, the first term is known, and the second term is unknown due to the unknown payload m_p. Also, $W(m_p,\dot{\bar{q}},\bar{q}) = 0$, if $m_p = 0$. In the following control design process, the influence of the unknown payload will not be considered in the baseline control law design process. Later, adaptive augmentations will be introduced to compensate for the disturbance caused by the payload. Hence, assuming that $m_p = 0$, the system equations of motion can be simplified to

$$\ddot{\bar{q}} = -\left[M_r^k(\bar{q})\right]^{-1}\left(C_r^k(\dot{\bar{q}},\bar{q})\dot{\bar{q}} + G_r^k(\bar{q}) + Q_r(\bar{q})\right). \tag{14}$$

Let $v_x = \dot{x}_q$, $v_z = \dot{z}_q$, $q = \dot{\theta}$, and $x = [x_q,\ z_q,\ \theta,\ v_x,\ v_z,\ q]^\top$. Let the control input be $u = [F,\ \tau]^\top$. The system equations of motion in Eq. (14) can be written in the state-space form as

$$\begin{bmatrix}\dot{x}_q\\ \dot{z}_q\\ \dot{\theta}\\ \dot{v}_x\\ \dot{v}_z\\ \dot{q}\end{bmatrix} = \left[\begin{array}{c} v_x\\ v_z\\ q\\ \hline -\left[M_r^k(x)\right]^{-1}\left(C_r^k(x)\dot{\bar{q}} + G_r^k(x) + Q_r(\bar{q})\right)\end{array}\right], \quad x(0) = x_0. \tag{15}$$

The vector field defined by the above presented equations of motion is nonlinear. Based on Eq. (14), the equilibrium point can be calculated as $\ddot{\bar{q}} = \dot{\bar{q}} = 0$, and hence we have

$$\ddot{x}_q = \ddot{z}_q = \ddot{\theta} = \dot{x}_q = \dot{z}_q = \dot{\theta} = v_x = v_z = q = \theta = 0.$$

This implies that $x_e = (x_q,\ z_q,\ 0,\ 0,\ 0,\ 0)$ is an equilibrium for any given $x_q, z_q \in \mathbb{R}$. The control input at the equilibrium is $u_e = (F_e,\ \tau_e)$ with

$$\begin{aligned}F_e &= (m_1 + m_2 + m_3)g,\\ \tau_e &= (m_2 l_{c1} + m_3 l_1)g\sin(\alpha) + m_3 l_{c2} g\sin(\alpha+\beta).\end{aligned} \tag{16}$$

For this vehicle, it is assumed that there will be no aggressive maneuvering, and the vehicle will be operating close to this equilibrium point. Hence the nonlinear dynamics in Eq. (14) can be linearized at the equilibrium for control

design purposes. Let $f(x) : \mathbb{R}^6 \to \mathbb{R}^6$ represent the vector field defined by Eq. (15). Then the linearized system can be obtained as

$$\dot{x} = Ax + Bu, \quad x(0) = 0, \tag{17}$$

where the system matrix and the input matrix are computed by

$$A = \left[\frac{\partial f(x)}{\partial x}\right]_{x=x_e,\ u=u_e}, \quad B = \left[\frac{\partial f(x)}{\partial u}\right]_{x=x_e,\ u=u_e}.$$

Symbolic calculations reveal that matrices A and B have the following forms:

$$A = \begin{bmatrix} 0 & 0 & 0 & 1 & 0 & 0 \\ 0 & 0 & 0 & 0 & 1 & 0 \\ 0 & 0 & 0 & 0 & 0 & 1 \\ 0 & 0 & -g & 0 & 0 & 0 \\ 0 & 0 & 0 & 0 & 0 & 0 \\ 0 & 0 & 0 & 0 & 0 & 0 \end{bmatrix}, \quad B = \begin{bmatrix} 0 & 0 \\ 0 & 0 \\ 0 & 0 \\ B_{41} & B_{42} \\ B_{51} & B_{52} \\ B_{61} & B_{62} \end{bmatrix},$$

and the matrix B is a function of the angles α and β. However, since the mass of link 1 and 2 is much smaller than the mass of the vehicle, the change of matrix B due to different manipulator configurations is small. Figure 3 shows the plots of nonzero elements of matrix B for different α and β such that $\alpha + \beta = \pi/2$, in which case, link 2 of the manipulator is always parallel to the x_1-axis of the body frame. Those plots also imply that the input F is most efficient as the control signal for $\dot{z}$, and the input τ is capable of controlling $\dot{\theta}$ efficiently, which is typical for a quadrotor.

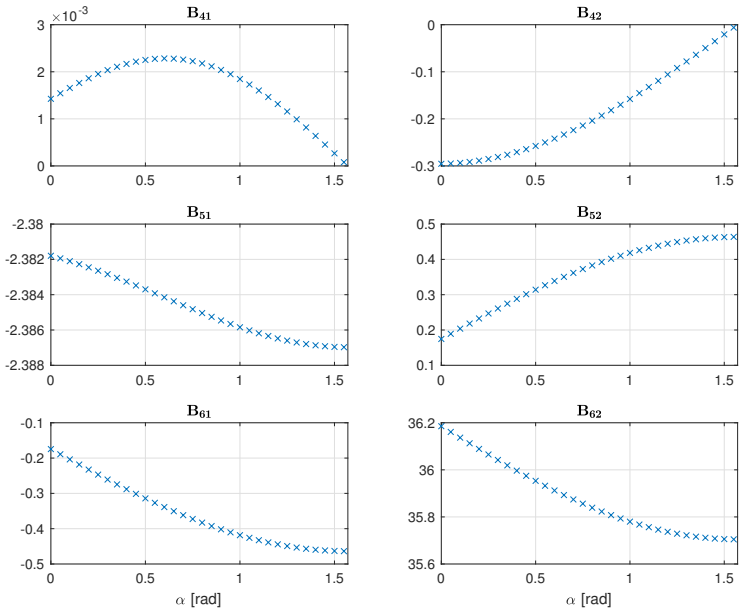

Fig. 3 Variation of nonzero elements in B matrix as α changes

Based on above analysis, the system can be decoupled into the following three subsystems and control laws will be designed for these three systems independently.

- Subsystem 1), horizontal translational dynamics:

$$\begin{aligned} \dot{x}_q &= v_x, \quad x_q(0) = x_{q0}, \\ \dot{v}_x &= -g\theta, \quad v_x(0) = v_{x0}. \end{aligned} \tag{18}$$

- Subsystem 2), vertical translational dynamics:

$$\begin{aligned} \dot{z}_q &= v_z, \quad z_q(0) = z_{q0}, \\ \dot{v}_z &= B_{51} F, \quad v_z(0) = v_{z0}. \end{aligned} \tag{19}$$

- Subsystem 3), rotational dynamics:

$$\begin{aligned} \dot{\theta} &= q, \quad \theta(0) = \theta_0, \\ \dot{q} &= B_{62} \tau, \quad q(0) = q_0. \end{aligned} \tag{20}$$

In the following, the influence of the unknown payload m_p on system equations will be explored to better understand the system. After adding an unknown payload, the overall mass and moment of inertia of the vehicle increase, leading to smaller magnitude of the element B_{51} and B_{62} in matrix B. To illustrate the effect of a payload, in Fig. 4 nonzero elements of matrix B are plotted for payloads of different mass. As the mass increases, the magnitudes of B_{51} and B_{62} decrease. In control law design, this uncertainty caused by the unknown payload has to be addressed carefully.

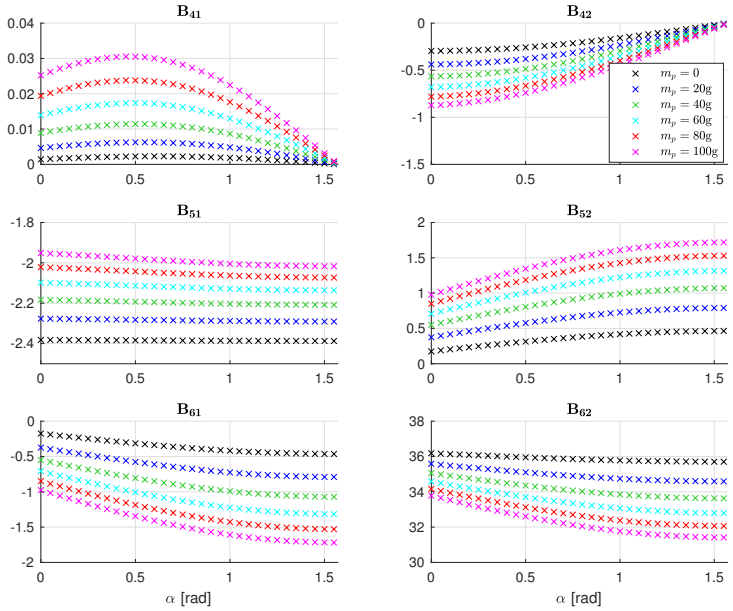

Fig. 4 Variation of nonzero elements in B matrix as α and m_p change

First, control laws will be designed for the rotational dynamics to achieve satisfactory pitch angle tracking performance. After that, a horizontal position tracking control law will be designed. Finally, the vertical position tracking control law will be developed. In the first and the last steps, a baseline control law will be designed first, based on which an adaptive controller will be augmented to compensate for the unknown payload and unknown configuration of the manipulator. The design configuration is chosen as $\alpha = \beta = \pi/4$ with $m_p = 0$.

B. General Control Structure

The control architecture consists of two position tracking controllers, a horizontal position tracking controller, and a vertical position tracking controller, which receive commands from either a vision-based pick-and-place controller or a trajectory generation module that generates position commands. The horizontal position tracking controller generates a pitch angle command for a pitch angle controller, which consists of a baseline pitch angle controller and an $\mathcal{L}_1$ adaptive augmentation. The vertical position tracking controller consists of a baseline position tracking controller and another $\mathcal{L}_1$ adaptive augmentation, which compensates for the unknown payload during pick-and-place. Figure 5 shows the general control structure of the system. In [5], a computed torque feedforward control law was developed to compensate for the

influence of the robot arm. However, the simulation results therein indicate that with the $\mathcal{L}_1$ adaptive augmentation, the feedforward control law is not necessary. Hence, in this study, the feedforward controller is not considered.

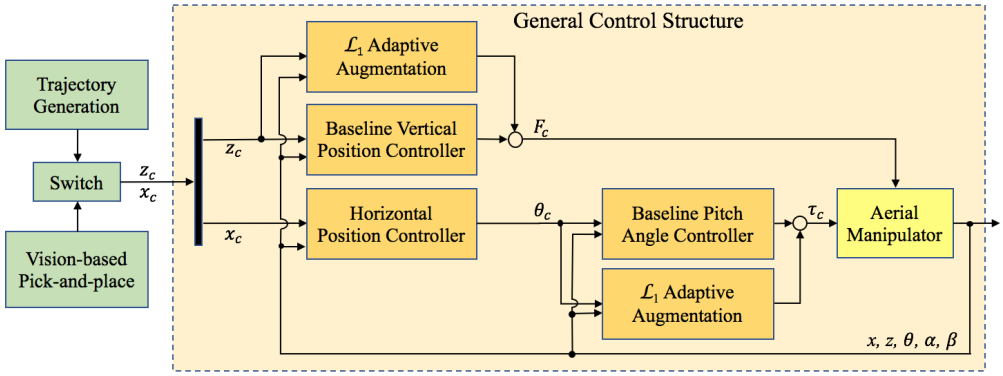

Fig. 5 General control structure

C. Horizontal Position Controller

In this subsection, the horizontal position controller will be developed. First, the baseline pitch angle controller design will be explained, followed by an adaptive augmentation. Then we present the horizontal position controller based on the pitch angle controller. The models used in this part are Subsystem 1) in Eq. (18) and Subsystem 3) in Eq. (20).

1. Baseline Pitch Angle Controller

The baseline pitch angle ($\theta(t)$) controller uses a PD control structure, which receives pitch angle command $\theta_c(t)$ from the horizontal position tracking control block. The control input $\tau_b(t)$ is given by

$$\tau_b(t) = K_p^\theta \left(\theta_c(t) - \theta(t)\right) + K_d^\theta q(t), \tag{21}$$

where K_p^θ and $K_d^\theta \in \mathbb{R}$ are control gains.

2. $\mathcal{L}_1$ Adaptive Augmentation for the Pitch Angle Controller

Similar to our previous study in [5], to compensate for the uncertainty introduced by the unknown payload m_p and different configurations of the manipulator arm an $\mathcal{L}_1$ adaptive control augmentation is developed with a piecewise constant adaptation law for the rotational motion of the vehicle.

The rotational dynamics of the vehicle with the baseline pitch angle control law in Eq. (21) and the $\mathcal{L}_1$ adaptive augmentation $u_a^\theta(t)$ can be written as

$$\begin{aligned} \dot{x}^\theta(t) &= A_m^\theta x^\theta(t) + B_r^\theta r^\theta(t) + B_m^\theta \left(u_a^\theta(t) + f_1^\theta(t, x^\theta)\right) + B_{um}^\theta f_2^\theta(t, x^\theta), \quad x^\theta(0) = x_0^\theta, \\ y^\theta(t) &= C_m^\theta x^\theta(t), \end{aligned} \tag{22}$$

where $x^\theta(t) = [\theta(t), q(t)]^\top$ is the vector of the measured system states, $r^\theta(t) = \theta_c(t)$ is the reference pitch angle command, $f_1^\theta(t, x^\theta) : \mathbb{R} \times \mathbb{R}^2 \to \mathbb{R}$ is a nonlinear function representing the matched uncertainty, which contains information on the unknown payload, the configuration of the manipulator, and the linearization residual, $f_2^\theta(t, x^\theta) : \mathbb{R} \times \mathbb{R}^2 \to \mathbb{R}$ is a nonlinear function representing additional modeling uncertainty. $A_m^\theta \in \mathbb{R}^{2\times 2}$ is a known Hurwitz matrix defining the desired system rotational dynamics, $B_r^\theta \in \mathbb{R}^{2\times 1}$ is the known command matrix, $B_m^\theta \in \mathbb{R}^{2\times 1}$ is the known input matrix, $C_m^\theta \in \mathbb{R}^{1\times 2}$ is a known vector, and $B_{um}^\theta \in \mathbb{R}^{2\times 1}$ is a matrix such that $B_m^{\theta\top} B_{um}^\theta = 0$ and $[B_m^\theta \; B_{um}^\theta]$ has full rank. The product $B_{um}^\theta f_2^\theta(t, x^\theta)$ represents the unmatched uncertainty. The matrices A_m^θ, B_r^θ, and B_m^θ are written as follows

$$A_m^\theta = \begin{bmatrix} 0 & 1 \\ -\bar{B}_{62} K_p^\theta & \bar{B}_{62} K_d^\theta \end{bmatrix}, \quad B_r^\theta = \begin{bmatrix} 0 \\ \bar{B}_{62} K_p^\theta \end{bmatrix}, \quad B_m^\theta = \begin{bmatrix} 0 \\ 1 \end{bmatrix},$$

where $\bar{B}_{62}$ is the nominal value of the element B_{62} for the design configuration $\alpha = \beta = \pi/4$ and $m_p = 0$. For the system given in Eq. (22), the following $\mathcal{L}_1$ adaptive controller is considered.

State Predictor: The state predictor takes the same structure as the system in Eq. (22) and is given by

$$\dot{\hat{x}}^\theta(t) = A_m^\theta \hat{x}^\theta(t) + B_r^\theta r^\theta(t) + B_m^\theta \left(u_a^\theta(t) + \hat{\sigma}_1^\theta(t)\right) + B_{um}^\theta \hat{\sigma}_2^\theta(t), \qquad \hat{x}^\theta(0) = x_0^\theta, \tag{23}$$

where $\hat{x}^\theta(t)$ is the observer state, $\hat{\sigma}_1^\theta(t) \in \mathbb{R}$ and $\hat{\sigma}_2^\theta(t) \in \mathbb{R}$ are the estimates of the nonlinear function $f_1^\theta(\cdot)$ and $f_2^\theta(\cdot)$ respectively.

Adaptation Law: Given an adaptation rate $T_s > 0$, the estimates $\hat{\sigma}_1^\theta(t)$ and $\hat{\sigma}_2^\theta(t)$ are updated according to the following piecewise constant adaptation law:

$$\begin{aligned} \begin{bmatrix} \hat{\sigma}_1^\theta(t) \\ \hat{\sigma}_2^\theta(t) \end{bmatrix} &= \begin{bmatrix} \hat{\sigma}_1^\theta(iT_s) \\ \hat{\sigma}_2^\theta(iT_s) \end{bmatrix}, \quad t \in [iT_s, (i+1)T_s) \\ \begin{bmatrix} \hat{\sigma}_1^\theta(iT_s) \\ \hat{\sigma}_2^\theta(iT_s) \end{bmatrix} &= -\begin{bmatrix} 1 & 0 \\ 0 & 1 \end{bmatrix} \left[B_m^\theta \; B_{um}^\theta\right]^{-1} \Phi_\theta^{-1}(T_s) e^{A_m^\theta T_s} \tilde{x}^\theta(iT_s), \quad i = 0, 1, 2, 3, \ldots, \end{aligned} \tag{24}$$

where

$$\Phi_\theta^{-1}(T_s) = \left(A_m^\theta\right)^{-1} \left(e^{A_m^\theta T_s} - \mathbb{I}_2\right),$$

and $\tilde{x}^\theta(t) = \hat{x}^\theta(t) - x^\theta(t)$ is the state prediction error.

Control Law: The control law is generated as the output of the following system:

$$u_a^\theta(s) = -k_a^\theta D^\theta(s) \hat{\eta}^\theta(s), \tag{25}$$

where $\hat{\eta}^\theta(s)$ is the Laplace transform of the signal

$$\hat{\eta}^\theta(t) \triangleq u_a^\theta(t) + \hat{\eta}_1^\theta(t) + \hat{\eta}_2^\theta(t)$$

with $\hat{\eta}_1^\theta(t) = \hat{\sigma}_1^\theta(t)$ and $\hat{\eta}_2^\theta(s) = H_{1\theta}^{-1}(s) H_{2\theta}(s) \hat{\sigma}_2^\theta(s)$ and

$$\begin{aligned} H_{1\theta}(s) &= C_m^\theta (s\mathbb{I} - A_m^\theta)^{-1} B_m^\theta, \\ H_{2\theta}(s) &= C_m^\theta (s\mathbb{I} - A_m^\theta)^{-1} B_{um}^\theta. \end{aligned}$$

Here k_a^θ is a feedback gain, and $D^\theta(s)$ is a strictly proper transfer function, which together lead to a strictly proper stable

$$C^\theta(s) \triangleq \frac{k_a^\theta D^\theta(s)}{1 + k_a^\theta D^\theta(s)}$$

with DC gain $C^\theta(0) = 1$.

3. Horizontal Position Controller

Based on the linearized dynamics in Eq. (18), the horizontal position ($x_q(t)$) controller also employs a PD control structure which receives horizontal position command $x_{qc}(t)$ from the upper level controller and generates a pitch angle command $\theta_c(t)$ for the lower level pitch angle tracking controller. The control input $\theta_c(t)$ is given by

$$\theta_c(t) = K_p^x \left(x_{qc}(t) - x_q(t)\right) + K_d^x v_x(t), \tag{26}$$

where K_p^x and $K_d^x \in \mathbb{R}$ are control gains. The total torque command sent the the system is then

$$\tau(t) = \tau_e + \tau_b(t) + u_a^\theta(t),$$

where τ_e, $\tau_b(t)$, and $u_a^\theta(t)$ are defined in Eqs. (16), (21), and (25) respectively.

D. Vertical Position Controller

The vertical position controller will be designed based on the dynamics in Eq. (19). It contains a baseline PD controller for the design configuration and an adaptive augmentation to compensate for modeling uncertainty and the unknown payload.

1. Baseline Vertical Position Controller

The following baseline force command is defined for vertical position control

$$F_b(t) = K_p^z \left(z_{qc}(t) - z_q(t)\right) + K_d^z v_z(t), \tag{27}$$

where K_p^z and $K_d^z \in \mathbb{R}$ are control gains.

2. $\mathcal{L}_1$ Adaptive Augmentation for the Vertical Position Controller

Similar to the design procedure of the adaptive augmentation for the pitch angle controller, we propose the following adaptive augmentation for the vertical position controller. The equations of vertical motion of the vehicle with the baseline vertical position control law in Eq. (27) and the $\mathcal{L}_1$ adaptive augmentation $u_a^z(t)$ can be written as

$$\begin{aligned} \dot{x}^z(t) &= A_m^z x^z(t) + B_r^z r^z(t) + B_m^z \left(u_a^z(t) + f_1^z(t, x^z)\right) + B_{um}^z f_2^z(t, x^z), \quad x^z(0) = x_0^z, \\ y^z(t) &= C_m^z x^z(t), \end{aligned} \tag{28}$$

where $x^z(t) = \left[z_q(t),\ v_z(t)\right]^\top$ is the vector of the measured system states, $r^z(t) = z_{qc}(t)$ is the reference altitude command, $f_1^z(t, x^z) : \mathbb{R} \times \mathbb{R}^2 \to \mathbb{R}$ is a nonlinear function representing the matched uncertainty, $f_2^z(t, x^z) : \mathbb{R} \times \mathbb{R}^2 \to \mathbb{R}$ is a nonlinear function representing additional modeling uncertainty. $A_m^z \in \mathbb{R}^{2\times 2}$ is a known Hurwitz matrix defining the desired vertical motion dynamics, $B_r^z \in \mathbb{R}^{2\times 1}$ is the known command matrix, $B_m^z \in \mathbb{R}^{2\times 1}$ is the known input matrix, $C_m^z \in \mathbb{R}^{1\times 2}$ is a known vector, and $B_{um}^z \in \mathbb{R}^{2\times 1}$ is a matrix such that $B_m^{z\top} B_{um}^z = 0$ and $[B_m^z\ B_{um}^z]$ has full rank. The product $B_{um}^z f_2^z(t, x^z)$ represents the unmatched uncertainty. The matrices A_m^z, B_r^z, and B_m^z are defined as follows

$$A_m^z = \begin{bmatrix} 0 & 1 \\ -\bar{B}_{51} K_p^z & \bar{B}_{51} K_d^z \end{bmatrix}, \quad B_r^z = \begin{bmatrix} 0 \\ \bar{B}_{51} K_p^z \end{bmatrix}, \quad B_m^z = \begin{bmatrix} 0 \\ 1 \end{bmatrix},$$

where $\bar{B}_{51}$ is the nominal value of the element B_{51} for the design configuration $\alpha = \beta = \pi/4$ and $m_p = 0$. For the system given in Eq. (28), the following $\mathcal{L}_1$ adaptive controller is proposed.

State Predictor: The state predictor has the same structure as the system in Eq. (28) and is defined by

$$\dot{\hat{x}}^z(t) = A_m^z \hat{x}^z(t) + B_r^z r^z(t) + B_m^z \left(u_a^z(t) + \hat{\sigma}_1^z(t)\right) + B_{um}^z \hat{\sigma}_2^z(t), \qquad \hat{x}^z(0) = x_0^z, \tag{29}$$

where $\hat{x}^z(t)$ is the observer state, $\hat{\sigma}_1^z(t) \in \mathbb{R}$ and $\hat{\sigma}_2^z(t) \in \mathbb{R}$ are the estimates of the nonlinear function $f_1^z(\cdot)$ and $f_2^z(\cdot)$ respectively.

Adaptation Law: Given the same adaptation rate $T_s > 0$, the estimates $\hat{\sigma}_1^z(t)$ and $\hat{\sigma}_2^z(t)$ are updated according to the following piecewise constant adaptation law:

$$\begin{aligned} \begin{bmatrix} \hat{\sigma}_1^z(t) \\ \hat{\sigma}_2^z(t) \end{bmatrix} &= \begin{bmatrix} \hat{\sigma}_1^z(iT_s) \\ \hat{\sigma}_2^z(iT_s) \end{bmatrix}, \quad t \in [iT_s, (i+1)T_s) \\ \begin{bmatrix} \hat{\sigma}_1^z(iT_s) \\ \hat{\sigma}_2^z(iT_s) \end{bmatrix} &= -\begin{bmatrix} 1 & 0 \\ 0 & 1 \end{bmatrix} \left[B_m^z\ B_{um}^z\right]^{-1} \Phi_z^{-1}(T_s) e^{A_m^z T_s} \tilde{x}^z(iT_s), \quad i = 0, 1, 2, 3, \ldots, \end{aligned} \tag{30}$$

where

$$\Phi_z^{-1}(T_s) = \left(A_m^z\right)^{-1} \left(e^{A_m^z T_s} - \mathbb{I}_2\right),$$

and $\tilde{x}^z(t) = \hat{x}^z(t) - x^z(t)$ is the state prediction error.

Control Law: The control law is generated as the output of the following system:

$$u_a^z(s) = -k_a^z D^z(s) \hat{\eta}^z(s), \tag{31}$$

where $\hat{\eta}^z(s)$ is the Laplace transform of the signal

$$\hat{\eta}^z(t) \triangleq u_a^z(t) + \hat{\eta}_1^z(t) + \hat{\eta}_2^z(t)$$

with $\hat{\eta}_1^z(t) = \hat{\sigma}_1^z(t)$ and $\hat{\eta}_2^z(s) = H_{1z}^{-1}(s)H_{2z}(s)\hat{\sigma}_2^z(s)$ and

$$H_{1z}(s) = C_m^z(s\mathbb{I} - A_m^z)^{-1}B_m^z,$$
$$H_{2z}(s) = C_m^z(s\mathbb{I} - A_m^z)^{-1}B_{um}^z.$$

Here k_a^z is a feedback gain, and $D^z(s)$ is a strictly proper transfer function, which together lead to a strictly proper stable

$$C^z(s) \triangleq \frac{k_a^z D^z(s)}{1 + k_a^z D^z(s)}$$

with DC gain $C^z(0) = 1$. The total force command sent to the system is then

$$F(t) = F_e + F_b(t) + u_a^z(t),$$

with F_e, $F_b(t)$, and $u_a^z(t)$ defined in Eqs. (16), (27), and (31) respectively.

IV. Simulations

A. Model Parameters

The parameters used in simulations are shown in Table 1. These parameters are based on a vehicle similar to the one, discussed in our previous work [5], and interested readers can find more details therein. The payload is assumed to be a cylinder.

Table 1 Vehicle parameters

m_1	380 g
m_2	10.1 g
m_3	29.9 g
l_1	100 mm
l_{c1}	43.5 mm
l_2	130 mm
l_{c2}	67.8 mm
I_{yy1}	2.70×10^{-2} kgm^2
I_{yy2}	2.87×10^{-5} kgm^2
I_{yy3}	1.89×10^{-4} kgm^2

B. Simulation Results

1. Pitch Angle Controller

Step responses of the baseline pitch angle controller are shown in Fig. 6. Figure 6a shows the step responses at the design configuration with $\alpha = \beta = \pi/4$. Figure 6b shows step responses of the baseline controller for a few different configurations. Since the mass of the arm is small, the configuration does not have a large effect on the dynamics, and hence similar performance is achieved. However, when there is a payload, the configuration will affect the influence of the payload on system dynamics, which will be shown in the following results.

When there is a payload, the dynamics of the system will change greatly. Step responses with different configurations are shown in Fig. 7. Figure 7a shows the response to a step command at time $t = 0$ s, while Fig. 7b shows the response to a step command at $t = 2$ s. The payload affects the performance of the baseline control law greatly. The payload caused the pitch angle to decrease at first. Then the pitch angle increased and settled to a value much smaller than the commanded value. With the adaptive augmentation, the influence of the payload was compensated for successfully, and the pitch angle converged to the commanded value; the performance for the design configuration was recovered. The

plot with the adaptive augmentation off also reveals the effect of the manipulator configurations. When α is larger, the payload is farther from the center of mass of the quadrotor, and hence a larger pitching moment will be generated by the payload, which increases the magnitude of the uncertainty. Without adaptive augmentation, the baseline control law cannot compensate for this disturbance. The payload picked up will cause the vehicle to tilt and hence fly forward. This should be avoided especially when the vehicle is picking up an item in front of a shelf or close to a wall. With adaptive augmentation, this problem can be solved.

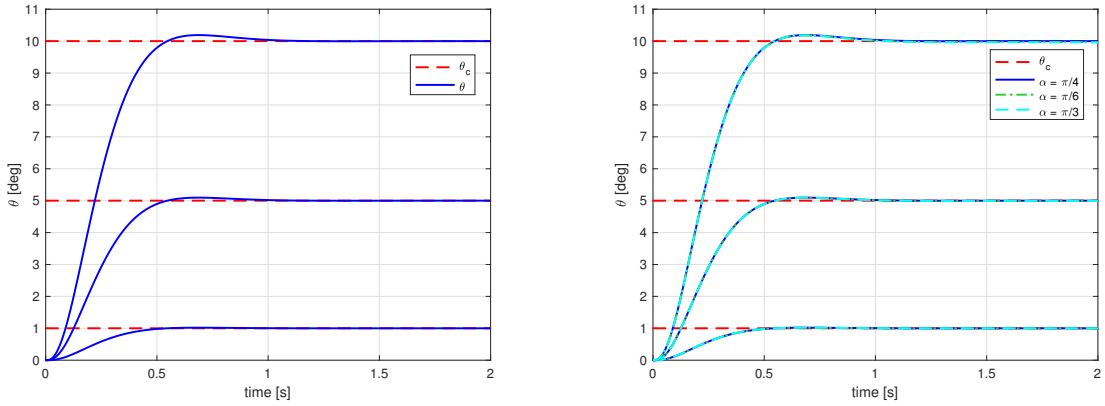

(a) Response at design configuration **(b) Response at other configurations**

Fig. 6 Step responses of the baseline pitch angle controller at different configurations

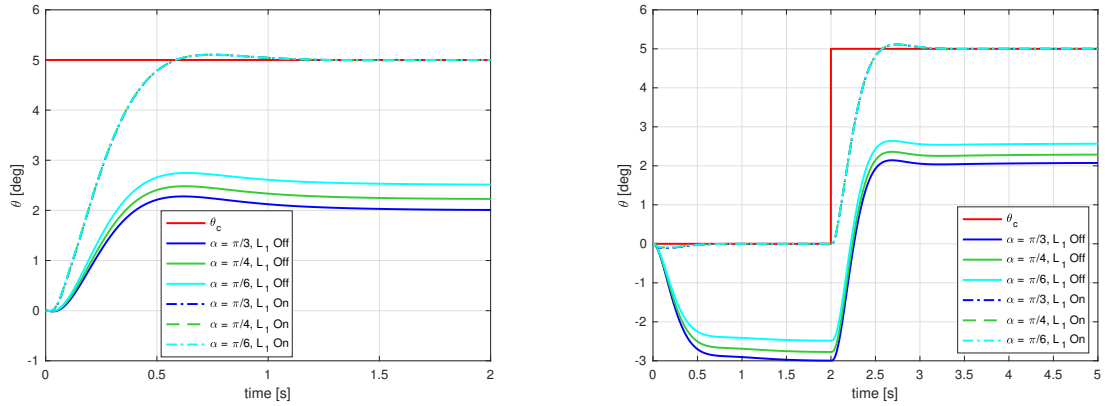

(a) Step command at $t = 0$ s **(b) Step command at $t = 2$ s**

Fig. 7 Step responses with payload at various configurations

2. Position Controllers

Step responses of the horizontal and the vertical position tracking controllers are shown in Fig. 8 and Fig. 9. Figure 8 shows the step response to the horizontal position command and the vertical position command respectively. Figure 9 shows the results, when there is a payload. The payload will affect both the horizontal and the vertical motion. It reduces the performance of both baseline position control laws. After the payload is picked up by the vehicle, the altitude of the vehicle will decrease, and the vehicle will move forward, which can be seen from Fig. 9b. The adaptive augmentation can compensate for this disturbance, and the vehicle moves according to the commands. This is important to achieve a safe and stable pick-and-place mission.

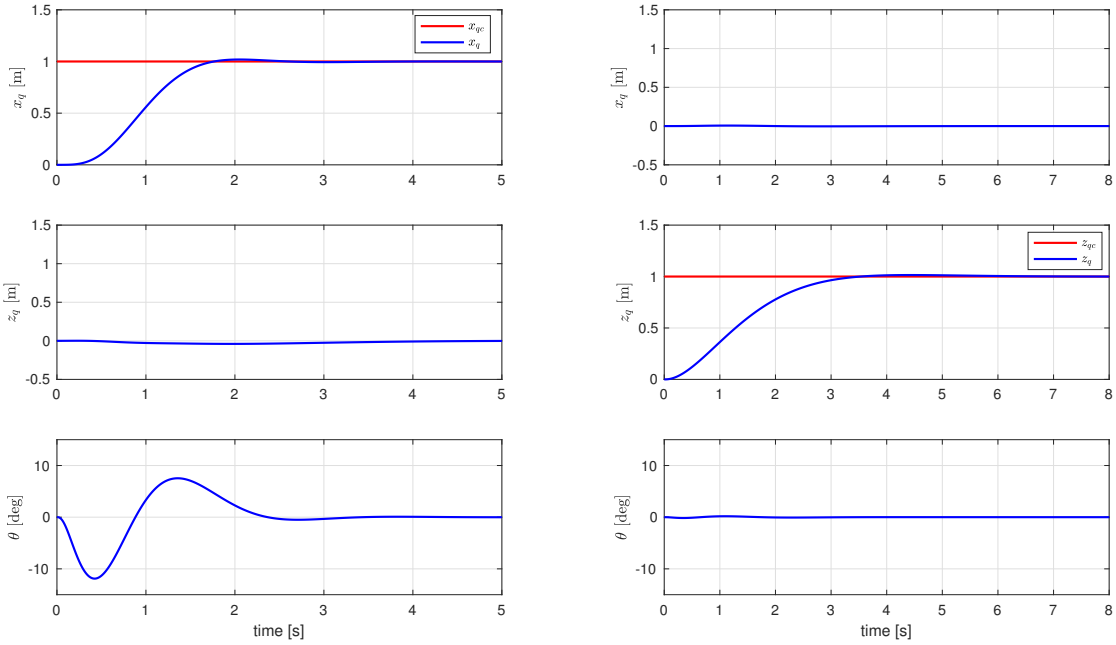

(a) Step response to x_q command **(b) Step response to z_q command**

Fig. 8 Step responses to position commands at design configuration without payload

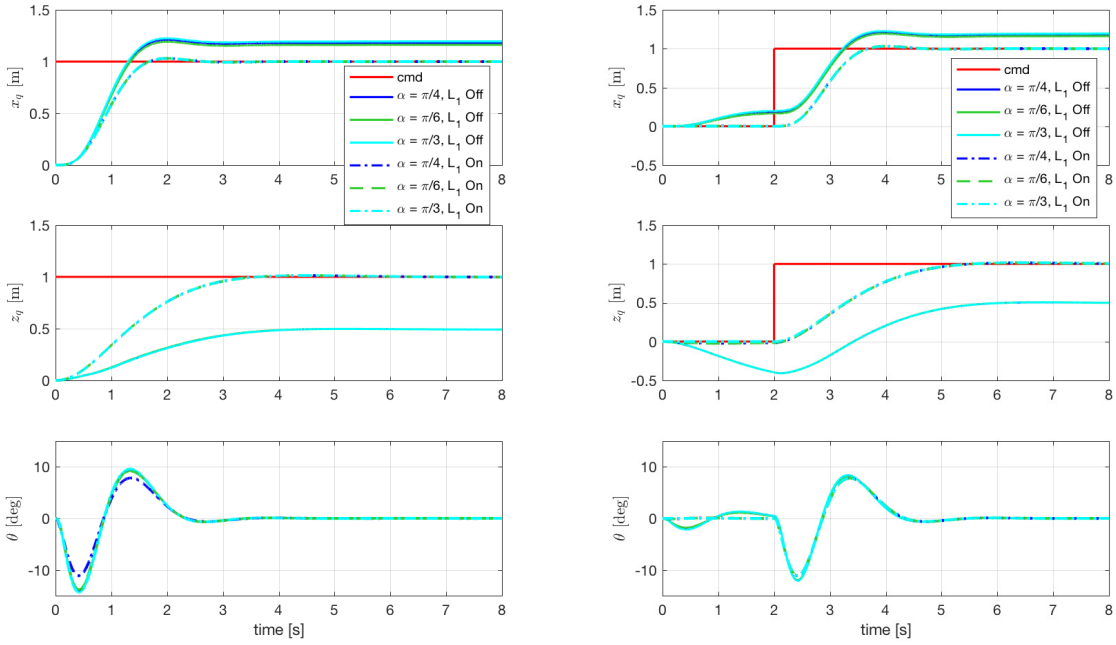

(a) Step command at $t = 0$ s **(b) Step command at $t = 2$ s**

Fig. 9 Step responses to position commands at different configurations with payload

In the following study, payload drop-off is simulated. Comparison is made between the performance with and without adaptive augmentations. Here only the configuration $\alpha = \beta = \pi/4$ is explored. Other configurations have similar results. A payload of mass $m_p = 30$ g was added to the manipulator at time zero, and then dropped off at time $t = 8$ s. The commanded positions are both zero in the horizontal and the vertical directions. Simulation results are shown in Fig. 10. Plots in Fig. 10a indicate that for the baseline control law, when the payload was dropped, the horizontal and vertical positions again underwent large changes. These changes are not desirable for the pick-and-place mission, especially when the vehicle is close to human users. With adaptive augmentations, the changes before and after the drop-off are much smaller, as shown in Fig. 10b. This behavior contributes to a more friendly human robot interaction.

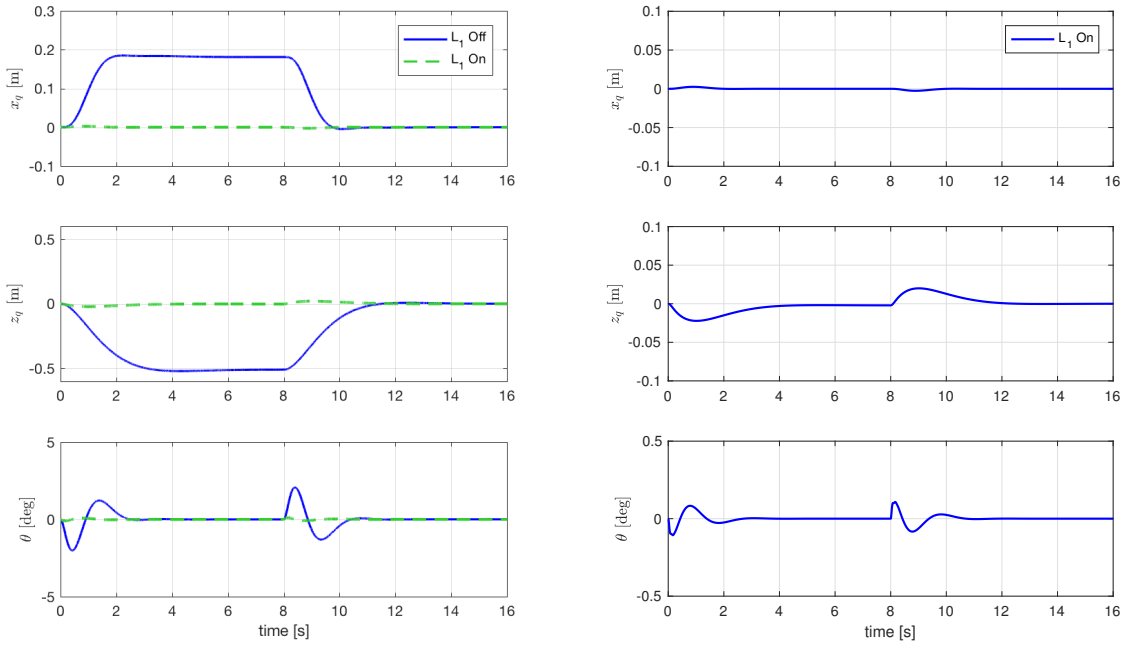

(a) Comparison of responses with $\mathcal{L}_1$ on and off

(b) Responses with $\mathcal{L}_1$ on

Fig. 10 Responses with a payload picked up at $t = 0$ s and dropped off at $t = 8$ s

V. Conclusion

This paper presented a control design for an aerial manipulator to facilitate the pick-and-place mission. The model of the vehicle was obtained using Lagrangian dynamics, which was then analyzed and linearized for control design purposes. A baseline pitch angle controller, a horizontal position controller, and a baseline vertical position controller have been developed using a PD control structure. Two $\mathcal{L}_1$ adaptive controllers were designed to augment the baseline pitch angle controller and the baseline vertical position controller to compensate for the influence of the payload picked up. Simulation examples verified the efficacy of the design. With an unknown payload, control performance for the design configuration without any payload can be recovered, which is critical to ensure that the vehicle will not deviate from the commanded positions after it picks up and drops off the payload. Future work will be conducted on the implementation of the proposed design on a real system and further flight test.

Appendix

The matrices $M(\bar{q})$, $C(\bar{q}, \dot{\bar{q}})$, and $G(\bar{q})$ are defined as follows

$$M(\bar{q}) = \left[\begin{array}{c|c|c|c|c} m_1+m_2+m_3+m_p & 0 & \begin{array}{l}(m_2l_{c1}+m_3l_1)\cos(\theta+\alpha)\\ +m_3l_{c2}\cos(\theta+\alpha+\beta)\\ +m_pl_1\cos(\theta+\alpha)\\ +m_pl_2\cos(\theta+\alpha+\beta)\end{array} & \begin{array}{l}(m_2l_{c1}+m_3l_1)\cos(\theta+\alpha)\\ +m_3l_{c2}\cos(\theta+\alpha+\beta)\\ +m_pl_1\cos(\theta+\alpha)\\ +m_pl_2\cos(\theta+\alpha+\beta)\end{array} & \begin{array}{l}m_3l_{c2}\cos(\theta+\alpha+\beta)\\ +m_pl_2\cos(\theta+\alpha+\beta)\end{array} \\ \hline 0 & m_1+m_2+m_3+m_p & \begin{array}{l}-(m_2l_{c1}+m_3l_1)\sin(\theta+\alpha)\\ -m_3l_{c2}\sin(\theta+\alpha+\beta)\\ -m_pl_1\sin(\theta+\alpha)\\ -m_pl_2\sin(\theta+\alpha+\beta)\end{array} & \begin{array}{l}-(m_2l_{c1}+m_3l_1)\sin(\theta+\alpha)\\ -m_3l_{c2}\sin(\theta+\alpha+\beta)\\ -m_pl_1\sin(\theta+\alpha)\\ -m_pl_2\sin(\theta+\alpha+\beta)\end{array} & \begin{array}{l}-m_3l_{c2}\sin(\theta+\alpha+\beta)\\ -m_pl_2\sin(\theta+\alpha+\beta)\end{array} \\ \hline \begin{array}{l}(m_2l_{c1}+m_3l_1)\cos(\theta+\alpha)\\ +m_3l_{c2}\cos(\theta+\alpha+\beta)\\ +m_pl_1\cos(\theta+\alpha)\\ +m_pl_2\cos(\theta+\alpha+\beta)\end{array} & \begin{array}{l}-(m_2l_{c1}+m_3l_1)\sin(\theta+\alpha)\\ -m_3l_{c2}\sin(\theta+\alpha+\beta)\\ -m_pl_1\sin(\theta+\alpha)\\ -m_pl_2\sin(\theta+\alpha+\beta)\end{array} & \begin{array}{l}I_{yy1}+I_{yy2}+I_{yy3}+I_{yyp}+m_2l_{c1}^2\\ +m_3(l_1^2+l_{c2}^2+2l_1l_{c2}\cos(\beta))\\ +m_p(l_1^2+l_2^2+2l_1l_2\cos(\beta))\end{array} & \begin{array}{l}I_{yy2}+I_{yy3}+I_{yyp}+m_2l_{c1}^2\\ +m_3(l_1^2+l_{c2}^2+2l_1l_{c2}\cos(\beta))\\ +m_p(l_1^2+l_2^2+2l_1l_2\cos(\beta))\end{array} & \begin{array}{l}I_{yy3}+I_{yyp}\\ +m_3(l_{c2}^2+l_1l_{c2}\cos(\beta))\\ +m_p(l_2^2+l_1l_2\cos(\beta)\end{array} \\ \hline \begin{array}{l}(m_2l_{c1}+m_3l_1)\cos(\theta+\alpha)\\ +m_3l_{c2}\cos(\theta+\alpha+\beta)\\ +m_pl_1\cos(\theta+\alpha)\\ +m_pl_2\cos(\theta+\alpha+\beta)\end{array} & \begin{array}{l}-(m_2l_{c1}+m_3l_1)\sin(\theta+\alpha)\\ -m_3l_{c2}\sin(\theta+\alpha+\beta)\\ -m_pl_1\sin(\theta+\alpha)\\ -m_pl_2\sin(\theta+\alpha+\beta)\end{array} & \begin{array}{l}I_{yy2}+I_{yy3}+I_{yyp}+m_2l_{c1}^2\\ +m_3(l_1^2+l_{c2}^2+2l_1l_{c2}\cos(\beta))\\ +m_p(l_1^2+l_2^2+2l_1l_2\cos(\beta))\end{array} & \begin{array}{l}I_{yy2}+I_{yy3}+I_{yyp}+m_2l_{c1}^2\\ +m_3(l_1^2+l_{c2}^2+2l_1l_{c2}\cos(\beta))\\ +m_p(l_1^2+l_2^2+2l_1l_2\cos(\beta))\end{array} & \begin{array}{l}I_{yy3}+I_{yyp}\\ +m_3(l_{c2}^2+l_1l_{c2}\cos(\beta))\\ +m_p(l_2^2+l_1l_2\cos(\beta)\end{array} \\ \hline \begin{array}{l}m_3l_{c2}\cos(\theta+\alpha+\beta)\\ +m_pl_2\cos(\theta+\alpha+\beta)\end{array} & \begin{array}{l}-m_3l_{c2}\sin(\theta+\alpha+\beta)\\ -m_pl_2\sin(\theta+\alpha+\beta)\end{array} & \begin{array}{l}I_{yy3}+I_{yyp}\\ +m_3(l_{c2}^2+l_1l_{c2}\cos(\beta))\\ +m_p(l_2^2+l_1l_2\cos(\beta))\end{array} & \begin{array}{l}I_{yy3}+I_{yyp}\\ +m_3(l_{c2}^2+l_1l_{c2}\cos(\beta))\\ +m_p(l_2^2+l_1l_2\cos(\beta))\end{array} & \begin{array}{l}I_{yy3}+I_{yyp}\\ +m_3l_{c2}^2+m_pl_2^2\end{array} \end{array}\right], \tag{32}$$

$$C(\dot{\bar{q}},\bar{q}) = \left[\begin{array}{cc|c|c|c} 0 & 0 & \begin{array}{l}-(\dot\theta+2\dot\alpha)(m_2l_{c1}+m_3l_1)\sin(\theta+\alpha)\\ -(\dot\theta+2\dot\alpha+2\dot\beta)m_3l_{c2}\sin(\theta+\alpha+\beta)\\ -(\dot\theta+2\dot\alpha)m_pl_1\sin(\theta+\alpha)\\ -(\dot\theta+2\dot\alpha+2\dot\beta)m_pl_2\sin(\theta+\alpha+\beta)\end{array} & \begin{array}{l}-\dot\alpha(m_2l_{c1}+m_3l_1)\sin(\theta+\alpha)\\ -(\dot\alpha+2\dot\beta)m_3l_{c2}\sin(\theta+\alpha+\beta)\\ -\dot\alpha m_pl_1\sin(\theta+\alpha)\\ -(\dot\alpha+2\dot\beta)m_pl_2\sin(\theta+\alpha+\beta)\end{array} & \begin{array}{l}-\dot\beta m_3l_{c2}\sin(\theta+\alpha+\beta)\\ -\dot\beta m_pl_2\sin(\theta+\alpha+\beta)\end{array} \\ \hline 0 & 0 & \begin{array}{l}-(\bar\theta+2\bar\alpha)(\bar m_2\bar l_{c1}+\bar m_3\bar l_1)\cos(\bar\theta+\bar\alpha)\\ -(\dot\theta+2\dot\alpha+2\dot\beta)m_3l_{c2}\cos(\theta+\alpha+\beta)\\ -(\dot\theta+2\dot\alpha)m_pl_1\cos(\theta+\alpha)\\ -(\dot\theta+2\dot\alpha+2\dot\beta)m_pl_2\cos(\theta+\alpha+\beta)\end{array} & \begin{array}{l}-\bar\alpha(\bar m_2\bar l_{c1}+\bar m_3\bar l_1)\cos(\bar\theta+\bar\alpha)\\ -(\dot\alpha+2\dot\beta)m_3l_{c2}\cos(\theta+\alpha+\beta)\\ -\dot\alpha m_pl_1)\cos(\theta+\alpha)\\ -(\dot\alpha+2\dot\beta)m_pl_2\cos(\theta+\alpha+\beta)\end{array} & \begin{array}{l}-\dot\beta m_3l_{c2}\cos(\theta+\alpha+\beta)\\ -\dot\beta m_pl_2\cos(\theta+\alpha+\beta)\end{array} \\ \hline 0 & 0 & 0 & 0 & \begin{array}{l}-(2\bar\theta+2\bar\alpha+\bar\beta)\bar m_3\bar l_1l_{c2}\sin(\bar\beta)\\ -(2\dot\theta+2\dot\alpha+\dot\beta)m_pl_1l_2\sin(\beta)\end{array} \\ \hline 0 & 0 & 0 & 0 & \begin{array}{l}-(2\bar\theta+2\bar\alpha+\bar\beta)\bar m_3\bar l_1l_{c2}\sin(\bar\beta)\\ -(2\dot\theta+2\dot\alpha+\dot\beta)m_pl_1l_2\sin(\beta)\end{array} \\ \hline 0 & 0 & \begin{array}{l}(\bar\theta+2\bar\alpha)\bar m_3\bar l_1l_{c2}\sin(\bar\beta)\\ +(\dot\theta+2\dot\alpha)m_pl_1l_2\sin(\beta)\end{array} & \begin{array}{l}\bar\alpha\bar m_3\bar l_1l_{c2}\sin(\bar\beta)\\ +\dot\alpha m_pl_1l_2\sin(\beta)\end{array} & 0 \end{array}\right], \quad G(\bar{q}) = \left[\begin{array}{c} 0 \\ \hline -(m_1+m_2+m_3+m_p)g \\ \hline \begin{array}{l}(m_2l_{c1}+m_3l_1+m_pl_1)g\sin(\theta+\alpha)\\ +(m_3l_{c2}+m_pl_2)g\sin(\theta+\alpha+\beta)\end{array} \\ \hline \begin{array}{l}(\bar m_2\bar l_{c1}+\bar m_3\bar l_1+\bar m_p\bar l_1)g\sin(\bar\theta+\bar\alpha)\\ +(m_3l_{c2}+m_pl_2)g\sin(\theta+\alpha+\beta)\end{array} \\ \hline (m_3l_{c2}+m_pl_2)g\sin(\theta+\alpha+\beta) \end{array}\right]. \tag{33}$$

Acknowledgments

This research was partially supported by the National Science Foundation NRI program, the China Scholarship Council, and the ZJU-UIUC Institute Research Program.

References

[1] Romer, G., Stuyt, H., and Peters, A., "Cost-Savings and Economic Benefits Due to the Assistive Robotic Manipulator (ARM)," *9th International Conference on Rehabilitation Robotics, 2005. ICORR 2005.*, Chicago, IL, USA, 2005.

[2] Tobe, F., "Where Are the Elder Care Robots?" IEEE Spectrum, Nov 2012. `http://spectrum.ieee.org/automaton/robotics/home-robots/where-are-the-eldercare-robots` [cited November 2018].

[3] Smarr, C.-A., Fausset, C. B., and Rogers, W. A., "Understanding the Potential for Robot Assistance for Older Adults in the Home Environment," Technical Report HFA-TR-1102, Human Factors and Aging Laboratory, Georgia Institute of Technology, 2011.

[4] Mitzner, T. L., Smarr, C.-A., Beer, J. M., Chen, T. L., Springman, J. M., Prakash, A., Kemp, C. C., and Rogers, W. A., "Older Adults' Acceptance of Assistive Robots for the Home," Technical Report HFA-TR-1105, Human Factors and Aging Laboratory, Georgia Institute of Technology, 2011.

[5] Jones, R. M., Sun, D., Haberfeld, G. B., Lakshmanan, A., Marinho, T., and Hovakimyan, N., "Design and Control of a Small Aerial Manipulator for Indoor Environments," *AIAA Information Systems-AIAA Infotech @ Aerospace*, 2017.

[6] Mellinger, D., Lindsey, Q., Shomin, M., and Kumar, V., "Design, modeling, estimation and control for aerial grasping and manipulation," *2011 IEEE/RSJ International Conference on Intelligent Robots and Systems*, San Francisco, CA, 2011.

[7] Spica, R., Franchi, A., Oriolo, G., Bulthoff, H. H., and Giordano, P. R., "Aerial grasping of a moving target with a quadrotor UAV," *2012 IEEE/RSJ International Conference on Intelligent Robots and Systems*, Vilamoura, Algarve, Portugal, 2012.

[8] Khalifa, A., Fanni, M., Ramadan, A., and Abo-Ismail, A., "Modeling and control of a new quadrotor manipulation system," *2012 First International Conference on Innovative Engineering Systems*, Alexandria, 2012.

[9] Thomas, J., Polin, J., Sreenath, K., and Kumar, V., "Avian-Inspired Grasping for Quadrotor Micro UAVs," *Volume 6A: 37th Mechanisms and Robotics Conference*, Portland, Oregon, 2013.

[10] Thomas, J., Loianno, G., Polin, J., Sreenath, K., and Kumar, V., "Toward autonomous avian-inspired grasping for micro aerial vehicles," *Bioinspir. Biomim.*, Vol. 9, No. 2, 2014.

[11] Orsag, M., Korpela, C., Bogdan, S., and Oh, P., "Lyapunov based model reference adaptive control for aerial manipulation," *2013 International Conference on Unmanned Aircraft Systems (ICUAS)*, Atlanta, GA, 2013.

[12] Bazylev, D., Margun, A., Zimenko, K., and Kremlev, A., "UAV equipped with a robotic manipulator," *22nd Mediterranean Conference on Control and Automation*, Palermo, Italy, 2014.

[13] Danko, T. W., Chaney, K. P., and Oh, P. Y., "A parallel manipulator for mobile manipulating UAVs," *2015 IEEE International Conference on Technologies for Practical Robot Applications (TePRA)*, Woburn, MA, 2015.

[14] Lee, H., Kim, S., and Kim, H. J., "Control of an aerial manipulator using on-line parameter estimator for an unknown payload," *2015 IEEE International Conference on Automation Science and Engineering (CASE)*, Gothenburg, Sweden, 2015.

[15] Garimella, G., and Kobilarov, M., "Towards model-predictive control for aerial pick-and-place," *2015 IEEE International Conference on Robotics and Automation (ICRA)*, Seattle, WA, 2015.

[16] Haberfeld, G. B., Sun, D., and Hovakimyan, N., "Stabilization and Optimal Trajectory Generation for a Compact Aerial Manipulation System with a Delta-type Parallel Robot," *2018 International Conference on Unmanned Aircraft Systems (ICUAS)*, 2018.

[17] Hovakimyan, N., and Cao, C., $\mathcal{L}_1$ *Adaptive Control Theory*, Society for Industrial and Applied Mathematics, Philadelphia, PA, 2010.

[18] Hovakimyan, N., Cao, C., Kharisov, E., Xargay, E., and Gregory, I. M., "$\mathcal{L}_1$ Adaptive Control for Safety-Critical Systems," *IEEE Control Systems Magazine*, Vol. 31, No. 5, 2011, pp. 54–104.

[19] Gregory, I. M., Xargay, E., Cao, C., and Hovakimyan, N., "Flight Test of $\mathcal{L}_1$ Adaptive Control Law: Offset Landings and Large Flight Envelope Modeling Work," *AIAA Guidance, Navigation, and Control Conference*, Portland, OR, 2011. AIAA 2011-6608.

[20] Ackerman, K., Xargay, E., Choe, R., Hovakimyan, N., Cotting, M. C., Jeffrey, R. B., Blackstun, M. P., Fulkerson, T. P., Lau, T. R., and Stephens, S. S., "L1 Stability Augmentation System for Calspan's Variable-Stability Learjet," *AIAA Guidance, Navigation, and Control Conference*, 2016.

[21] Ackerman, K. A., Xargay, E., Choe, R., Hovakimyan, N., Cotting, M. C., Jeffrey, R. B., Blackstun, M. P., Fulkerson, T. P., Lau, T. R., and Stephens, S. S., "Evaluation of an L1 Adaptive Flight Control Law on Calspan's Variable-Stability Learjet," *Journal of Guidance, Control, and Dynamics*, Vol. 40, No. 4, 2017, pp. 1051–1060.

[22] Henderson, H. V., and Searle, S. R., "On Deriving the Inverse of a Sum of Matrices," *SIAM Review*, Vol. 23, No. 1, 1981, pp. 53–60.